WATER CHEMISTRY CONTROL AS CORROSION MITIGATION STRATEGY

M. MOLINARI[1], E. LO PICCOLO[2], R. TORELLA[2], M. D'ONORIO[1], N. TERRANOVA[3], G. CARUSO[1]

[1]Sapienza University of Rome, Rome, Italy
[2]RINA Consulting – Centro Sviluppo Materiali S. p. A., Castel Romano, Rome, Italy
[3]ENEA Fusion and Technology for Nuclear Safety and Security Department, Frascati, Italy

Email contact of corresponding author: martina.molinari@uniroma1.it

1. INTRODUCTION

During the operative phase of a cooling circuit of a fusion Nuclear Power Plant (NPP), several phenomena entail the variation of the corrosion rate. The production of Corrosion Products (CPs) poses a radiological issue in a nuclear fusion power plant since the neutron field from the burning plasma has enough energy to activate both the surrounding materials and their CPs. It is well known from the literature that Activated CPs (ACPs) constitute a relevant issue in terms of Occupational Radiation Exposure (ORE), source term during accidental scenarios, waste management, and maintenance planning [1,2,3,4,5].

Considering the Water Cooled Lithium Lead (WCLL) blanket concept of the EUropean DEMOnstrator fusion NPP (EU-DEMO), the corrosion and erosion phenomena occur throughout the piping system, both within the coolant loop and in the breeding material. However, for the purposes of this study, only water-induced corrosion will be addressed.

Corrosion phenomena are electrochemical processes typically divided into two stages. The initial stage involves material degradation due to exposure to a specific environment. In contrast, the second stage consists of the recombination of degradation by-products with the constituents of the environment. As outlined in [6], numerous types of corrosion exist, commonly categorized as wet or dry. In a water-cooled fusion NPP, wet corrosion is prevalent due to water in the coolant loop within the piping system. Consequently, optimizing water chemistry becomes an effective method for mitigating corrosion phenomena. Both uniform and localized corrosion can compromise the material's structural integrity, leading to a range of impacts. For instance, increased circulation of corrosion products in a cooling circuit can amplify radiological contamination within the circuit. Simultaneously, high corrosion rates can trigger incidental events such as pitting, leading to Loss Of Coolant Accidents or crevice corrosion that can result in the failure of flanged connections.

In a fusion reactor, an alkalizing agent needs to be added to the cooling circuit's water chemistry to counteract acidification, a condition that can arise from radiolysis or increased temperatures [7]. Furthermore, maintaining an inert atmosphere is necessary to prevent the creation of an oxidizing environment or the solution's carbonation. Different experimental analyses have been performed to collect data about the corrosion behavior of different alloys, such as the EUROFER and the Stainless Steel 316L, under specific environmental conditions using Potassium Hydroxide (KOH) as a base. The choice of KOH as a base comes from the experience of the successful pH control in Water Water Energetic Reactor (VVER) designs, but its compatibility with western PWRs has rarely been investigated. The replacement of Lithium Hydroxide (LiOH) with KOH in PWR primary water was completed by the Electric Power Research Institute (EPRI) in 2002 [7].

The experimental approach used in this study aligns with the methodology applied in [8], where experimental activities were designed to validate various water chemistry compositions for fusion NPPs, specifically using Lithium Hydroxide (LiOH) and Ammonia (NH3) as bases.

This study presents the outcomes from six distinct expositions, each executed with two primary objectives: pH stabilization and observation of localized corrosion phenomena.

2. EXPERIMENTAL CAMPAIGN

The six tests were performed in RINA-CSM's laboratories, using a corrosion loop tailored explicitly for the experimental conditions replicating those of the EU-DEMO WCLL Primary Heat Transfer System. The test apparatus is a corrosion loop test named High-Pressure High-Temperature (HPHT), which comprises an autoclave shown in Fig.1, a heat exchanger, and a pumping system. The heat exchanger cools the solution from 300°C to 25°C while the pumping system propels the solution at 2 m/s. Prior to re-entering the autoclave, the solution is pre-heated to 100°C.

The tests conducted are outlined in Table 1. Each solution was based on Ultrapure Water but varied in KOH concentrations (ranging from 5 ppm to 52 ppm) and oxygen concentrations (spanning from less than 10 ppb to 300 ppb). Regardless of these variations, each test maintained consistent 100 bar and 300 °C conditions, with a fluid velocity set at 2 m/s.

Multiple specimens of EUROFER and SS316L were tested in each trial. All specimens were hot rolled flat coupons with standardized dimensions of 20x20x3 mm and were allocated into the autoclave as represented in Fig. 2. Each test ran for up to 1000 hours.

Water chemistry was meticulously optimized for every test to achieve neutrality conditions throughout the test period.

FIG. 1. Autoclave (2.5 l) of the experimental loop.

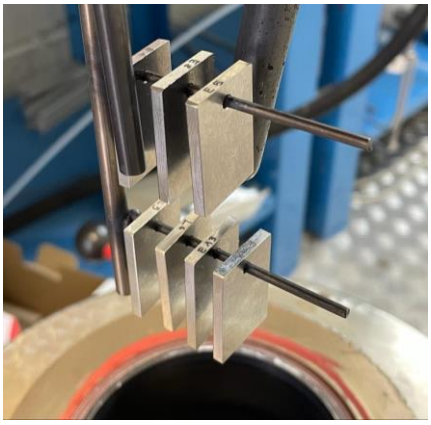

FIG. 2. Allocation of the specimens.

TABLE 1. TESTS PERFORMED

Test N.	Solution	O_2 [ppb]	Specimen type	Pressure [bar]	Temperature [°C]	Time [h]	Aim
1	KOH (5 ppm)	< 10	EUROFER SS316L	100	300	1000	Looking for pH stability
2	KOH (26 ppm)	< 10	EUROFER SS316L	100	300	1000	
3	KOH (52 ppm)	< 10	EUROFER SS316L	100	300	1000	
4	KOH (52 ppm)	100	EUROFER	100	300	1000	Looking for localized phenomena
5	KOH (52 ppm)	200	EUROFER SS316L	100	300	1000	
6	KOH (52 ppm)	300	EUROFER SS316L	100	300	1000	

During the setting up of the test apparatus, a small sample of the solution was extracted to measure the initial pH. The pH measurements were conducted in an air environment during both the pre-test and post-test phases for all experiments. For Test 1, Test 2, and Test 3, samples were taken weekly to construct a time-dependent pH graph. All the specimens were degreased with acetone and weighed prior to their placement in the autoclave.

3. RESULTS

Each post-test analysis followed a consistent procedure. The corrosion rate was determined based on the weight loss of the samples, adhering to the ASTM G1 procedure [9]. Furthermore, the oxide scale was characterized using Scanning Electron Microscopy (SEM) and Energy Dispersive X-ray Spectroscopy (EDX or EDS). A comprehensive water chemistry analysis was also carried out for each test.

In terms of pH stability, as demonstrated in Fig.3, a more stable pH at 25°C was achieved with a KOH concentration of 52 ppm. This specific concentration was subsequently chosen to manage the solution's oxygen content.

Each specimen was weighed before the test, before and after the pickling treatment with a solution of hydrogen chloride (HCl) and hexamethylenetetramine (HMTA), at the end of each test. The corrosion rates of the specimens are summarized in Table 2.

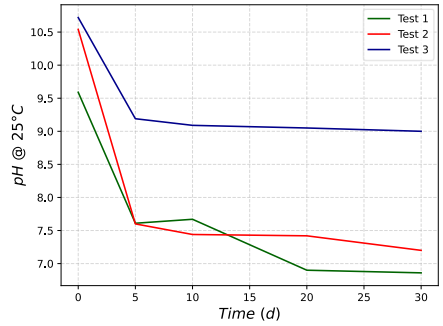

FIG. 3. pH trend

TABLE 2. CORROSION RATES

Test N.	Material	Corrosion Rate w/o pickling treatment [µm/y]	Corrosion rate with pickling treatment (HCl + HMTA) [µm/y]
1	EUROFER	3.0 ÷ 3.2	7.6
	SS316L	0.1 ÷ 0.2	1
2	EUROFER	1.9 ÷ 2.6	5.1
	SS316L	0.3 ÷ 0.4	1
3	EUROFER	0.0992 ÷ 0.1045	0.2325 ÷ 0.2625
4	EUROFER	0.0058 ÷ 0.069	0.0464 ÷ 0.1598
	SS316L	0.0086 ÷ 0.0201	0.023
5	EUROFER	0.1336 ÷ 0.1689	0.2497 ÷ 0.3081
	SS316L	0.0057 ÷ 0.0171	0.0228 ÷ 0.0229
6	EUROFER	0.0148 ÷ 0.1035	0.0148 ÷ 0.1568
	SS316L	0.0059 ÷ 0.0266	0.0059 ÷ 0.0266

After evaluating the corrosion rates, the oxide scale was characterized by SEM and EDS analyses. Fig. FIG. *4*, FIG. 5, Fig. FIG. *6*, and Fig. FIG. *7* show the EUROFER oxide scale with a sectional view of the specimen. The photos are in Back Scattering Electron (BSE or BEC) mode because, as explained in [10], the BSE can show a compositional image instead of the Secondary Electrons (SE or SEC), which show only a higher resolution image but not compositional.

The oxide scale comprises chromium and iron oxide in all the analyzed specimens with EDS. The chromite is the first layer on the surface of the materials. Instead, the magnetite is a second layer above the chromite layer, which is formed below the 100°C as described in [11], and is a protection for the EUROFER material, which is not stainless. The difference between the two layers is visible in FIG. 5, FIG. 6 in the section view, and FIG. 8 and FIG. 9.

No localized corrosion phenomena have been detected during the post-test analysis of any tests.

During the EDS analysis, the adherent corrosion layer thickness has also been measured, and values are summarized in Table 3.

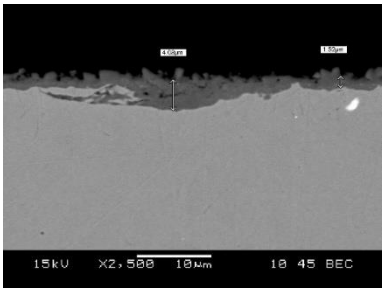

FIG. 4. Test 3 – 10000 X BSE, section.

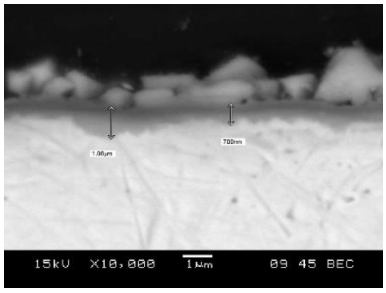

FIG. 5. Test 4 – 10000 X BSE, section.

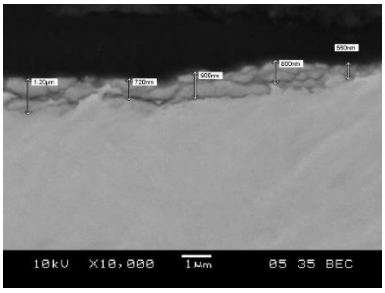

FIG. 6. Test 5 -10000 X BSE, section.

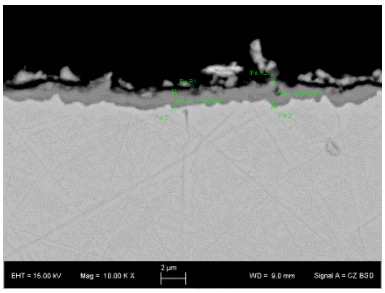

FIG. 7. Test 6 – 10000 X BSE, section.

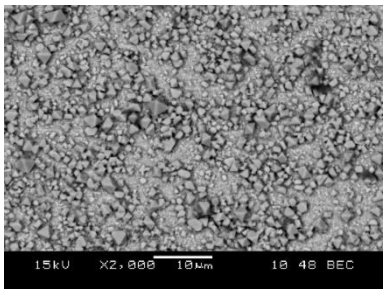

FIG. 8. Test 4 – 2000 X BSE, surface.

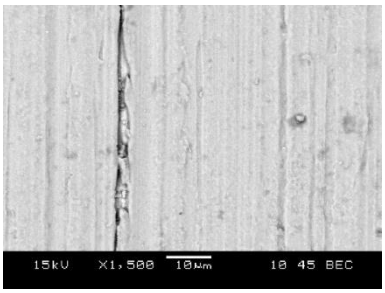

FIG. 9. Test 5 – 1500 X BSE, surface.

TABLE 3. ADHERENT CORROSION LAYER THICKNESS

Test n.	Thickness [um]
3	1.52 ÷ 4.08
4	0.70 ÷ 1.06
5	0.560 ÷ 1.20
6	1.346 ÷ 2.078

The water chemistry analysis was performed at the end of each test to assess the concentration of releases of different elements and the pH value at the beginning and end of the tests. The results of the water chemistry analysis are reported in Table 4.

TABLE 4. WATER CHEMISTRY ANALYSIS

Test N.	Fe [ppb]	Cr [ppb]	Ni [ppb]	Co [ppb]	Mo [ppb]	Cu [ppb]	W [ppb]	pH_{in} T=23°C	pH_{fin} T=23°C
1	36	0.3	5	<0.01	38	6	<0.01	9.59	6.86
2	42	3	41	<0.01	315	<0.5	5	10.54	7.20
3	113	15.5	21.2	0.36	246	5.3	18.0	10.72	9
4	68	3.6	14.4	<0.1	296	1.91	7.71	10.82	9.32
5	50.0	1.43	1.63	0.05	144.4	6.72	11.64	10.91	9.33
6	20.0	2.68	6.26	0.05	180.2	5.12	14.85	10.62	9.48

4. DISCUSSION AND CONCLUSIONS

The impact of water chemistry on corrosion and release phenomena was investigated through experimental activities featuring two distinct analysis phases. The first phase focused on achieving stable pH levels, monitored persistently at the beginning and conclusion of the tests and through intermittent sampling during the testing process. The second phase of analysis focused on conducting tests with variable oxygen levels, with the pH already stabilized.

The concentration of KOH in the water solution was optimized to foster a more stable pH trend. As mentioned earlier, control of oxygen content was only performed in the test where the KOH concentration was 52 ppm due to its enhanced pH stability. The results from tests both with and without pickling treatment indicated a significant divergence in corrosion rates when the KOH concentration was increased to 52 ppm. Tests 1 and 2 exhibited near-neutral pH levels when the solution was cooled down to 25 °C. However, this subsequently led to the acidification of the solution when heated to 300 °C. A noteworthy impact on pH was also identified when studying the outcomes of the oxygen control tests. The corrosion rates of Tests 4, 5, and 6 (both with and without pickling treatment) were much lower than those of Tests 1, 2, and 3, even though the oxygen concentration was significantly lower. Oxygen control in the water solution was performed to identify a threshold above which localized phenomena occur under these specific environmental conditions. However, no localized phenomena were observed.

This conclusion was reinforced by examining both surfaces and sectional views using an optical microscope and SEM. It can be seen from Table 2 the significant difference in corrosion rates before and after the pickling treatment. This difference is a sign that magnetite has been developed as expected, which has actually worked as a protective layer, avoiding the formation of localized phenomena.

The absence of localised corrosion indicates that, in the absence of radiolysis, an initial oxygen concentration of about 300 ppb does not imply more severe structural damage with respect to uniform corrosion. Future experimental analyses will focus on investigating the threshold value beyond which localized corrosion phenomena occur.

REFERENCES

[1] DI PACE, L., QUINTINIERI, L., Assessment of Activated Corrosion Products for the DEMO WCLL, Fus. Eng. Des., (2018) 1168-1172.

[2] TERRANOVA, N., Activation Corrosion Products (ACP) Assessment, Report IDM, EDFA_D_XYZ123, EUROfusion, Garching, Germany, 2020.

[3] TERRANOVA, N., ACPs Assessment for DEMO Divertor Cooling Loop, Report IDM EDFA_D_2P9QUG, EUROfusion, Garching, Germany, 2022.

[4] INTERNATIONAL ATOMIC ENERGY AGENCY, Reactor Water Chemistry Relevant to Coolant-Cladding Interaction, IAEA-TECDOC-429, (1987).

[5] NUCLEAR ENERGY AGENCY, Radiation Protection Aspects of Primary Water Chemistry and Source-term Management, NEA/CRPPH/R(2014)2, NEA, 2014.

[6] FONTANA, M. G., Corrosion Engineering, Third Edition, McGraw-Hill Book Company, Singapore (1987).

[7] MACDONALD, D. D., ENGELHARDT, G. R., PETROV, A., A Critical Review of Radiolysis Issues in Water Cooled Fission and Fusion Reactors: Part I, Assessment of Radiolysis Models, Corr. Mater. Degrad., (2022) 470-535.

[8] FRUZZETTI, K., "Potassium Hydroxide (KOH) Qualification Program – Overview", EPRI-NRC Research Discussion on KOH Qualification, EPRI, 2017.

[9] LO PICCOLO, E., TORELLA, R., TERRANOVA, N., DI PACE, L., GASPARRINI, C., DALLA PALMA, M., Preliminary assessment of cooling water chemistry for fusion power plants, Corr. Mater. Degrad., (2021) 512-530.

[10] AMERICAL SOCIETY FOR TESTING AND MATERIALS, Standard Practice for Preparing, Cleaning, and Evaluating Corrosion Test Specimens, ASTM G1-03(2017)e1, ASTM, 2017.

[11] WELLS, O. C., "Scanning Electron Microscope", Encyclopedia of Materials: Science and Technology, Second Edition, Elsevier, Netherlands, 2001.

[12] TURNER, C. W., "Formation of corrosion products of carbon steel under condenser operating conditions", paper presented at Nuclear Plant Chemistry Conference (NPC), Paris (France), 2012.